OXFORD Toxicology Research

Toxicology Research, 2021, **10**, 376–388

doi: 10.1093/toxres/tfab018
Advance Access Publication Date: 12 April 2021
Paper

PAPER

Promotion effects of DEHP on hepatocellular carcinoma models: up-regulation of PD-L1 by activating the JAK2/STAT3 pathway

Qiang Xu,[1,†] Song Huang,[1,†] Zi-Ming Xu,[2] Ke Ji,[1] Xiang Zhang,[3] Wei-Ping Xu[3,*] and Wei Wei[1,*]

[1]Key Laboratory of Anti-inflammatory and Immune Medicine of Education Ministry, Anhui Collaborative Innovation Center of Anti-inflammatory and Immune Medicine, Institute of Clinical Pharmacology of Anhui Medical University, No. 81 Meishan Road, Hefei, Anhui 230032, China, [2]The Second Affiliated Hospital of Anhui Medical University, No. 678 Furong Road, Hefei, Anhui 230601, China and [3]Division of Life Sciences and Medicine, Anhui Provincial Key Laboratory of Tumor Immunotherapy and Nutrition Therapy, The First Affiliated Hospital of USTC, University of Science and Technology of China, No 17 Lujiang Road, Hefei, Anhui 230001, China

*Correspondence address. Division of Life Sciences and Medicine, Anhui Provincial Key Laboratory of Tumor Immunotherapy and Nutrition Therapy, The First Affiliated Hospital of USTC, University of Science and Technology of China, Hefei, Anhui 230001, China. Tel: +86 0551 6228 3106; Fax: +86 0551 6228 3106; E-mail: xu_weiping666@163.com (W.-P. Xu); Correspondence may also be addressed to Key Laboratory of Anti-inflammatory and Immune Medicine of Education Ministry, Anhui Collaborative Innovation Center of Anti-inflammatory and Immune Medicine, Institute of Clinical Pharmacology of Anhui Medical University, Hefei, Anhui 230032, China. Tel: +86 0551 6516 1209; Fax: +86 0551 6516 1209; E-mail: wwei@ahmu.edu.cn (W. Wei)
†Contribute equally to the manuscript.

Abstract

Di(2-ethylhexyl) phthalate (DEHP), as an endocrine disruptor, is often used as a plasticizer in various polyvinyl chloride plastic products and medical consumables. Epidemiological studies have shown that long-term large intake of DEHP may be a risk factor for liver dysfunction. Long-term exposure to DEHP is associated with liver disease and aggravates the progression of chronic liver injury. However, the effects of DEHP on hepatocellular carcinoma (HCC) are rarely studied. In this study, we sought to determine the effects of DEHP on HCC induced by carbon tetrachloride combined with diethylnitrosamine, and further study its molecular mechanism. It was found that DEHP exposure significantly promotes tumor immune escape and activates signaling pathways involved in related protein expression of tumor immune escape, including PD-L1, JAK2, and STAT3. In addition, the trends observed in the HepG2 cells assay are consistent with vivo conditions. In summary, DEHP may play a tumor-promoting role in HCC mice and IFN-γ stimulated HepG2 cells, which may be related to the JAK2/STAT3 signaling pathway.

Key words: DEHP, PD-L1, tumor immune escape, hepatocellular carcinoma (HCC), JAK2, STAT3

Received: 19 November 2020; **Revised:** 3 February 2021; **Accepted:** 10 February 2021

Introduction

Phthalates (PAEs) are organic chemical, one of the most commonly used plasticizers, widely used in plastic products, industrial, and household products [1, 2]. Since phthalates are bonded to plastic polymers with non-covalent bonds, they can easily leak into the environment. The main routes of exposure to these substances are ingestion, inhalation, skin absorption, or intravenous administration [3, 4]. Although there are many reports on the toxicity of Di(2-ethylhexyl) phthalate (DEHP), it is still widely used in consumer products and some medical devices, such as personal care products, plastics, packaging goods, cosmetics, blood bags, infusion tubes, nasogastric tube, peritoneal dialysis bag, and urinary catheter [5, 6]. In recent years, with the widespread use of phthalate-containing products, the toxicity of DEHP has attracted the attention of the scientific community. Studies have shown that DEHP is an environmental endocrine disrupting substance. Long-term exposure to DEHP will have a variety of effects on the human body, including liver toxicity, reproductive toxicity, neurotoxicity, carcinogenicity, immunotoxicity, etc. [7, 8].

Nowadays, the incidence of liver cancer continues to rise worldwide, and it has become an important health problem facing people. Liver cancer is the fifth most common cancer in the world and the third leading cause of cancer-related deaths. In most countries, mortality is almost equal to morbidity, which indicates that liver cancer lacks effective prevention and treatment [9]. Hepatocellular carcinoma (HCC) is the main type of primary liver cancer, accounting for 75–85% of all cases [10]. Many risk factors are related to the occurrence of liver cancer, including hepatitis B and C infections, alcohol consumption, obesity, nonalcoholic fatty liver disease, diethylnitrosamine (DEN), aflatoxin and as well as drinking water blue-green algae toxins, etc. [11]. The treatment methods for HCC mainly include surgical resection, chemotherapy, radiation therapy, interventional therapy, liver transplantation, and so on [12–14].

Tumor immune escape refers to the phenomenon that tumor cells grow and metastasize by avoiding the recognition and attack of the immune system through various mechanisms. It is an important strategy for tumor survival and development. There are many inducing factors for tumor immune escape, including low immunogenicity of tumor cells. Tumor-specific antibodies are recognized as autoantigens, tumor surface antigen regulation, tumor-induced immune exempt areas, tumor-induced immune suppression, etc. [15]. Programmed death ligand 1 (PD-L1) is a known ligand of programmed death 1 (PD-1), which is expressed on various cells including tumors and immune cells [16]. In tumor biology, the PD-1/PD-L1 pathway is an adaptive immune escape mechanism for tumor cells to respond to endogenous anti-tumor activity. When PD-L1 expressed on tumor cells binds to PD-1 receptors on immune cells, this interaction leads to inhibition of the proliferation, survival, and effector functions of CD8+ cytotoxic T lymphocytes, thereby inducing apoptosis of tumor-infiltrating T cells [17, 18]. In some tumor types, the expression level of PD-L1 is positively correlated with the degree of tumor metastasis and invasion [19].

Previous studies have shown that high-dose DEHP exposure can mediate liver oxidative damage by increasing TGF-β1/Smad and p38MAPK/NF-κB, thereby aggravating the development of liver fibrosis [20]. These results indicate that DEHP exposure has the ability to stimulate liver toxicity or chronic liver injury. However, the effects of DEHP on HCC are rarely studied. The purpose of this study is to explore whether DEHP can aggravate HCC by increasing the expression of PD-L1, and to explore its possible molecular mechanism.

Materials and methods

Animals and experimental design

The wild-type male mice were purchased from the Experimental Animal Center of Anhui Medical University and have a pure C57BL/B6 background. All mice were placed in a standard 12-h light/dark cycle and fed a standard rodent diet at the Animal Center of Anhui Medical University. The animals used in this study were approved by the Animal Experiment Ethics Evaluation Committee of the Institute of Clinical Pharmacology, Anhui Medical University. Fifteen-day-old mice were injected by DEN (25 mg/kg). When the mice were 4-weeks old, olive oil containing 10% carbon tetrachloride (CCl_4) was injected intraperitoneally twice a week at a dose of 5 µl/g. Seventy two mice were randomly allocated into six groups (12 mice/group) and were treated as follows: Group 1 (control) were served as a vehicle control and intraperitoneal injection of olive oil. Group 2 (HCC Model) intraperitoneal injection of DEN and CCl_4. The animals in Groups 3, 4, and 5 were served as exposure groups, intraperitoneal injection with DEN, CCl_4, and DEHP at 0.1, 10, and 1000 mg/kg. The animals in Group 6 were only given 1000 mg/kg of DEHP. When mice were 18 weeks old, mice are deprived of food for 12–24 h, after anesthetizing with ether, blood, and liver samples were collected for further study.

For experimental purposes, we chose the "real world" DEHP concentration range. We selected three doses of 0.1, 10, and 1000 mg/kg to study the effects of DEHP on HCC. In our study, the low dose of 0.1 mg/kg is the daily dose we can obtain from food, water, and other aspects of daily life. The median dose of 10 mg/kg is close to a specific occupation categories (such as plastic factory workers) and the patient's exposure dose. A high dose of 1000 mg/kg may cause significant liver toxicity.

Body weight, relative liver weight, tumor number, and tumor size of mice

The mice were anesthetized with 10% chloral hydrate (3 ml/kg), the blood was collected in a test tube and centrifuged (1500 × *g*, 10 min, 4°C). The plasma is stored at −80°C until described below. The liver was quickly dissected and washed with 0.9% saline (1:9, w:v). The liver was weighed and the liver index was calculated (liver weight/body weight ×100). Finally, some liver tissues were fixed with 4% paraformaldehyde for routine histopathological examination, and the remaining liver specimens were kept at −80°C. The number of tumors is observed by naked eyes, and the size is measured by vernier calipers.

AST and ALT activities in serum samples

Taken mouse blood, let it standed at room temperature for 2 h, and then centrifuged at 4°C and 3000 r/min for 10 min, collected the supernatant, and stored it at −80°C. A commercial test kit (Nanjing Jiancheng Institute of Biological Engineering, Nanjing) was used to detect the activity of serum aspartate aminotransferase (AST) (U/L) and alanine aminotransferase (ALT) (U/L).

Assay of alpha fetoprotein AFP

According to the kit instructions (Abcam, British ab210969 mouse alpha-fetoprotein), enzyme-linked immunosorbent assay (ELISA) technology was used to quantitatively determine serum

alpha-fetoprotein (AFP). The lowest detectable limit is 287 pg/ml. The linearity is up to 60 ng/ml.

Liver histopathological analysis

Samples of liver were extracted from mice in every group after 24 h, fixed in 10% formaldehyde for more than 48 h for histopathological examination. The fixed liver tissues were dehydrated in graded ethanol and embedded in paraffifin. Each paraffifin block was processed into 5-μm-thick slices and stained with hematoxylin and eosin. Perform hematoxylin quality and eosin (H&E) staining for routine morphological evaluation.

ELISA analysis

ELISA kits for TNF-α and IL-6 were purchased from R&D System (R&D, USA). Measure the levels of TNF-α and IL-6 using an ELISA kit according to the manufacturer's instruction. Measure TNF-α and IL-6 in liver tissue with an enzyme-linked immunosorbent assay (ELISA) kit. When the stop solution changes the color from blue to yellow, use a microplate reader (Winooski, VT, USA) to detect at 450 nm to the intensity of the color. The concentration of the sample was compared with the standard curve to determine the concentration of TNF-α and IL-6 in the sample. When the sample concentration exceeds the limit of the standard deviation value, it needs to be measured after dilution.

Distribution and expression of PD-L1 protein in liver tissues were detected by laser scanning confocal microscopy

First, the paraffin sections were placed in an oven at 60°C for 1.5 h, and then deparaffinized and hydrated in graded xylene and ethanol. Then wash three times with PBS, then soak in 0.5% Triton X-100 for 30 min, cover with EDTA antigen retrieval solution for 10 min, and block the sections in 5% BSA for 1 h at room temperature and then the anti-mouse PD-L1 antibody were incubated at 4°C, over night. After re-warming at 4°C, the sections were washed three times with PBS, and the sections were incubated with goat anti-mouse Alexa Fluor 594 secondary antibody at 25°C for 1 h in the dark. Finally, DAPI (Beyotime) was dropped on the slices, the nuclei were counter-stained for 10 min, washed with PBS three times, fixed with a fluorescence quencher, and observed with laser scanning confocal microscopy (LSCM).

In vitro experimental design and treatment

Liver cancer cell line (HepG2) was obtained from China Cell Culture Center (Shanghai, China). The cells were cultured in DMEM medium (HyClone, USA) containing 10% fetal bovine serum (FBS), while adding 100 units/ml penicillin and 100 μg/ml streptomycin to inhibit bacterial growth. The cells were incubated at 37°C and 5% CO_2. When the cells are cultured to the logarithmic growth phase, each experiment is performed.

Determination of cell viability by cck-8

The well-growing HepG2 cells were cultured in DMEM containing 10% FBS for 12 h in a 96-well plate with a density of 1×10^4 cells/well. When the concentration of IFN-γ is 30 ng/ml, the expression of PD-L1 is more obvious. They were divided into eight groups: normal control group, IFN-γ (30 ng/ml) and IFN-γ with 6.25, 12.5, 25, 50, 100, 200 μmol/l DEHP group for 24 h, and each group had five duplicate wells [20, 21]. After 24 h of DEHP treatment, CCK-8 solution (BestBio) was added to each well, each well was 10 μl, and the cells were continuously cultured for 1–4 h at 5% CO_2 and 37°C. The optical densities (ODs) of each inspection hole is measured at 450 nm test wavelength.

Table 1: Primer sequence for real-time PCR assay

Gene		Primer sequence
PD-L1	Forward	GACCACCACCACCAATTCCAAGAG
	Reverse	TGGAGGATGTGCCAGAGGTAGTTC
GAPDH	Forward	CAGGAGGCATTGCTGATGAT
	Reverse	GAAGGCTGGGGCTCATTT

Table 2: Body weight of mice in each group

Group dose (mg/kg)	Body weight (g)
Control	29.65 ± 1.19
Model (DEN + CCl_4)	24.89 ± 1.28**
DEN + CCl_4 + DEHP0.1 mg/kg	23.32 ± 1.46
DEN + CCl_4 + DEHP10 mg/kg	22.83 ± 1.03***
DEN + CCl_4 + DEHP1000 mg/kg	22.12 ± 2.36***
DEHP 1000 mg/kg	22.89 ± 1.05**

Date represent the mean ± SD.
*$P < 0.05$.
**$P < 0.01$ vs. control group.
***$P < 0.05$.
****$P < 0.01$ vs. DEN + CCl_4 group.

Detection of PD-L1 mRNA expression by RT-PCR

Take logarithmic growth phase HepG2 cells, inoculate 1×10^6 cells per well in a 6-well plate, and set the following six groups: normal control group, IFN-γ (30 ng/ml), IFN-γ (30 ng/ml) with 12.5, 50, 200 μmol/l DEHP group and a separate DEHP 200 μmol/l. After 24 h of DEHP treatment, the cells were washed twice with PBS, RNA was extracted with trizol reagent, and $A_{260/280}$ and its concentration were measured with a microplate reader. Follow the instruction of the reverse transcription kit to prepare the system to reverse transcribe RNA into cDNA. The reaction parameters are 50°C, 30 min, 85°C, 15 min. Configure the reaction system according to the real-time PCR kit and proceed with the reaction. The reaction parameters are 95°C, 15 s; 60°C, 30 s; 72°C, 30 s. Among them, pre-denaturation at 95°C for 2 min, a total of 40 cycles. The sequence of the gene primers is shown in Table 1.

Detection of the effects of DEHP on HepG2 cell migration by Transwell

Take logarithmic growth phase HepG2 cells, inoculate 1×10^5 cells per well in a 12-well plate, and set the following six groups: normal control group, IFN-γ (30 ng/ml), IFN-γ (30 ng/ml) with 12.5, 50, 200 μmol/l DEHP group and a separate DEHP 200 μmol/l. After culturing for 24 h, adjust the concentration of HepG2 cells

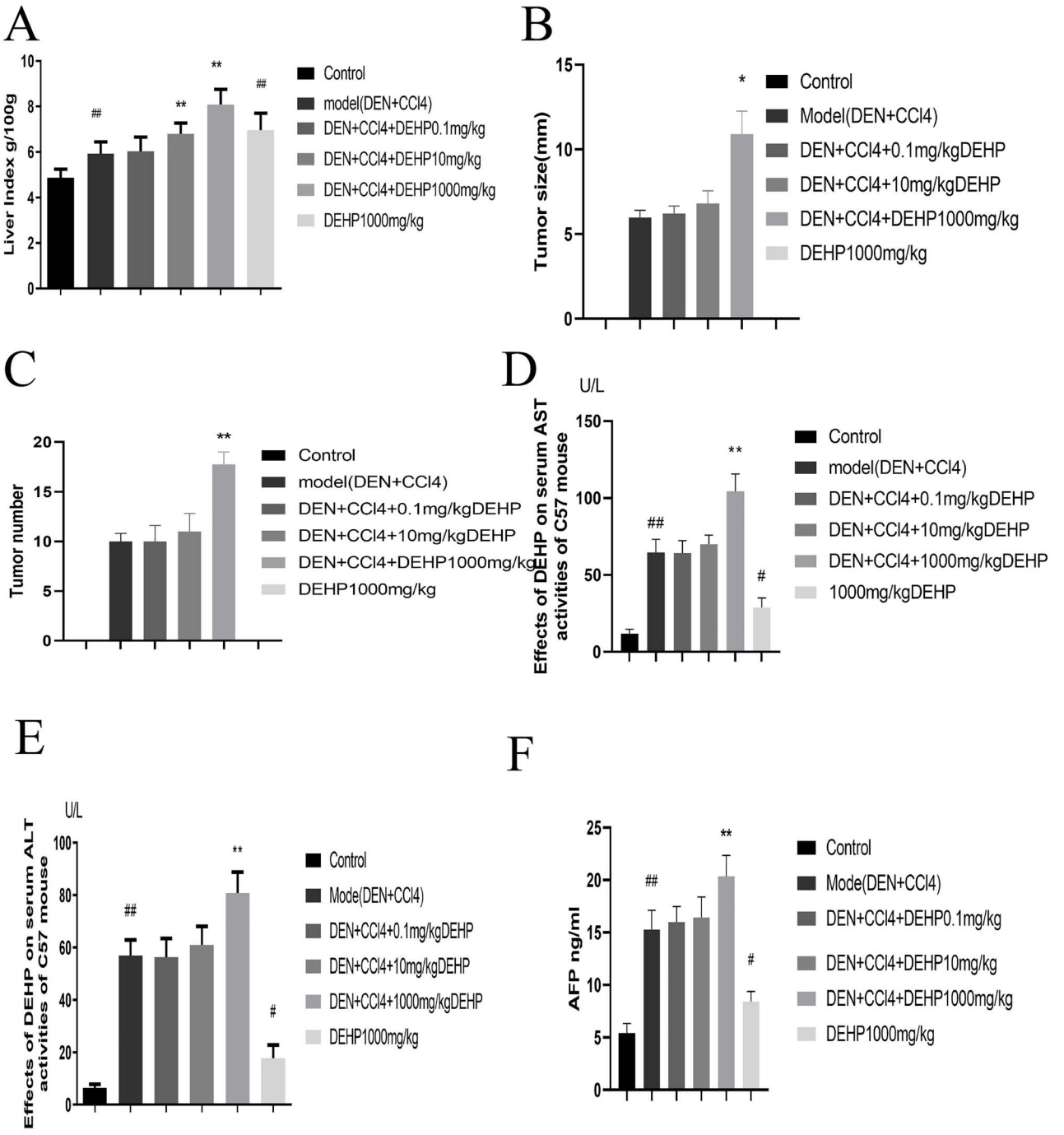

Figure 1: (**A**) Changes of liver index in mice after DEHP intervention ($n = 10$). (**B**, **C**) Measurement of tumor burdens. (**D**, **E**) The effects of DEHP on the activity of serum AST and ALT in C57BL/6 mice. (**F**) DEHP increased the level of AFP (Date represent the mean ± SD, #$P < 0.05$, ##$P < 0.01$ vs. control group, *$P < 0.05$, **$P < 0.01$ vs. model group).

again to 5 × 10^5/ml, add 200 µl per well to the upper chamber of the 24-well Transwell chamber, and add medium without FBS to the upper chamber. And add 30% FBS to the lower chamber of the Transwell chamber. After 24 h, take out the Transwell chamber used in the migration experiment, wipe off the cells that have not passed through the upper chamber with a cotton swab, wash with PBS three times, and then stain with crystal violet for 15 min, wipe the upper chamber with the cotton swab, and place the upper chamber observe under an electron microscope and take pictures.

Distribution and expression of PD-L1 protein in HepG2 cells were detected by laser scanning confocal microscopy

The HepG2 cells in logarithmic growth phase were treated with DEHP for 24 h, and then subjected to cellular immunofluorescence experiments. First, wash the wave plate in the 24-well plate with PBS three times, then fix the cells with 4% pre-chilled paraformaldehyde for 30 min. After washing once with PBS, add 0.5% Triton X-100 to the cells for 10 min. After washing with PBS, add 1% BSA to block at room temperature for 30 min, wash with

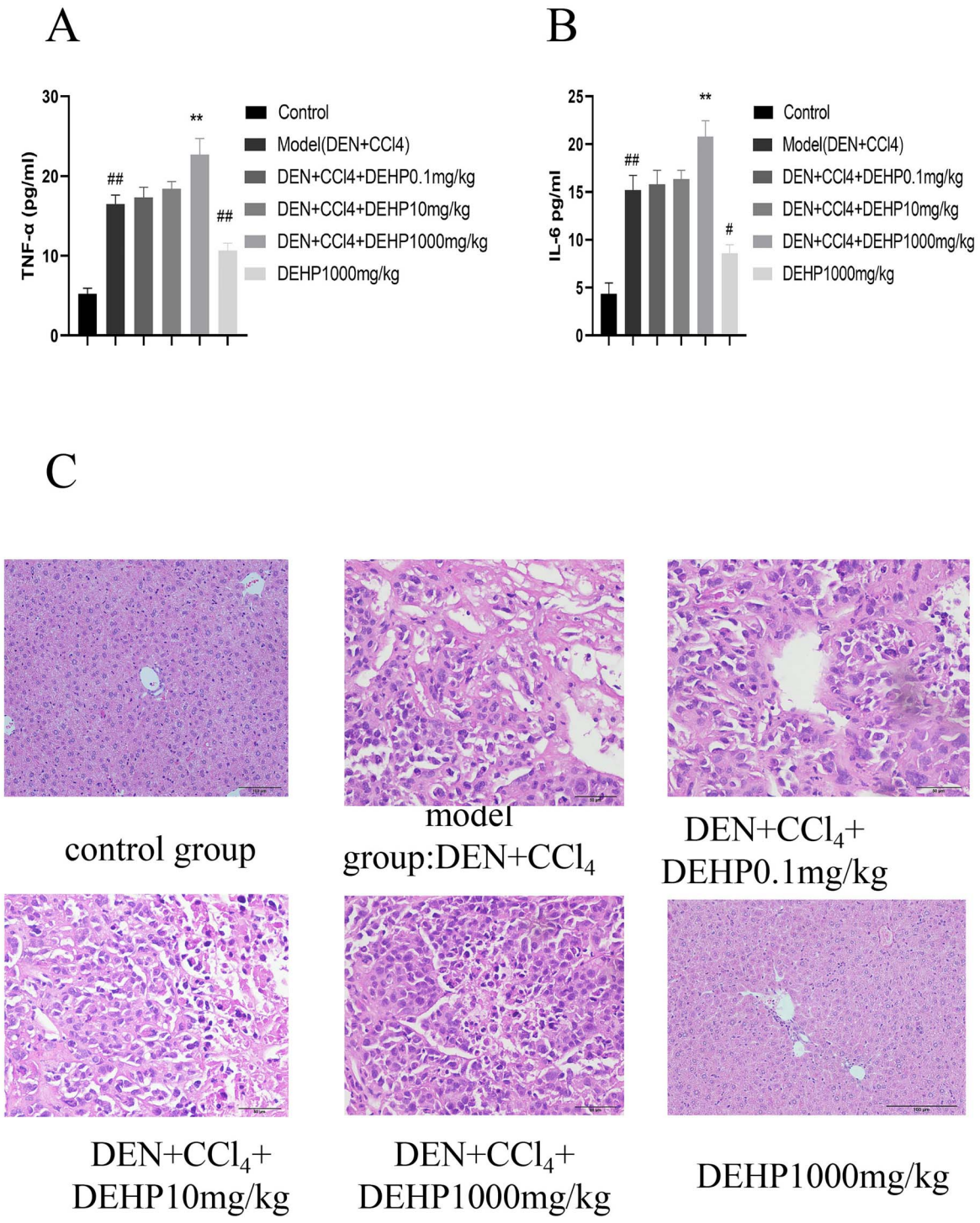

Figure 2: (**A**, **B**) The effects of DEHP on serum IL-6 and TNF-α levels in HCC mice. (**C**) DEHP promotes the occurrence and development of primary liver cancer in mice induced by DEN combined with CCl_4. H&E staining to observe liver histological changes (400×).

PBS three times, and then incubate the wave plate with anti-mouse PD-L1 antibody at 4°C overnight. After re-warming at 4°C, the wave plate was washed three times with PBS, and then incubated with goat anti-mouse Alexa Fluor 594 secondary antibody in the dark at room temperature for 1 h. Finally, DAPI was added dropwise and incubated for 5 min in the dark, and then mounted with a fluorescence quencher, and observed with LSCM.

The expression of PD-L1, P-JAK2, and P-STAT3 were analyzed by western blot

First, RIPA mixture containing protease inhibitor and phosphatase inhibitor is used to dissolve liver tissue and cells, and extract protein. Second, use the BCA protein quantification kit (China Biyuntian) to detect protein level. The protein in the sample was separated by SDS-PAGE and transferred to

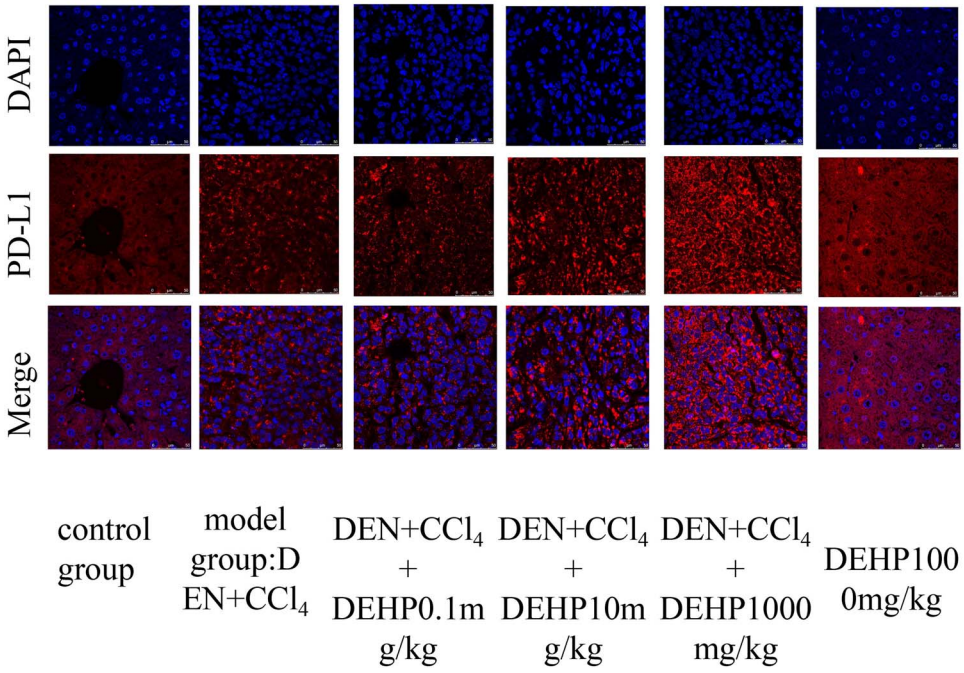

Figure 3: LSCM for PD-L1 protein expression and distribution in liver tissue, the PD-L1 is showed is red color, the nucleus blue color with DAPI.

a PVDF membrane (Millipore, Billerica, MA, USA). Then, the PVDF membrane was incubated with TPBS containing 5% skim milk, and incubated at 37°C for about 2 h. After blocking, the PVDF membrane was incubated with the specific primary antibody at 4°C overnight. On the second day, wash the incubated membrane with TPBS 3 times, and then incubate in horseradish peroxidase-conjugated anti-rabbit antibody and anti-mouse antibody (1:10 000) at 37°C for about 1 h. After 1 h, the membrane was washed three times with TPBS and once with PBS. The protein bands were detected by an enhanced chemiluminescence reaction and exposed to Image Quant LAS 4000 mini. Densitometry analysis of specific bands was performed by Image J software.

Statistical analysis

All experimental data were expressed as mean ± standard deviation (SD), and graphpad Prism v 8.0 was used to draw histograms. SPSS 25.0 software was used for statistical analysis of multiple data in each group. The comparison of multiplexed data from the experimental group was analyzed by one-way analysis of variance and Duncan test. Values of $P < 0.05$ were considered statistically significant.

Results

The effects of DEHP on body weight, relative liver weight, tumor number, and tumor size in mice

As shown in Table 2, compared with the control group, the weight of the model group was significantly reduced. Compared with the model group, the weight of the DEHP 0.1 mg/kg group did not change significantly, while the weight of the DEHP 10, 1000 mg/kg group decreased. Compared with the control group, the weight of the DEHP 1000 mg/kg control group was significantly reduced. As shown in Figure 1A, compared with the control group, the liver index of the model group increased significantly; compared with the model group, the liver index of the DEHP 0.1 mg/kg group did not change significantly, and the liver index of the DEHP 10, 1000 mg/kg group was significantly increased. Compared with the control group, the liver index of the DEHP 1000 mg/kg control group increased significantly. As shown in Figure 1B and C, compared with the model group, the tumor size and number in the DEHP 0.1, 10 mg/kg group did not change significantly, while the tumor size and number in the DEHP 1000 mg/kg control group increased.

The effects of DEHP on the activities of serum AST and ALT in mice

The activity levels of mice serum AST and ALT are used as biochemical indicators of liver injury. The results shown in Figure 1D and E show that compared with the control group, the serum AST and ALT activity levels of the model group increased significantly; compared with the model group, the ALT and AST levels of the DEHP 0.1 mg/kg group did not change significantly, while the ALT and AST levels of the DEHP10, 1000 mg/kg group increased significantly. Compared with the control group, the AST and ALT activity levels of the DEHP 1000 mg/kg control group increased significantly.

The effects of DEHP on serum AFP level in mice

AFP is a specific tumor marker for diagnosing primary liver cancer, which has the function of establishing diagnosis, early diagnosis and differential diagnosis [22]. Figure 1F shown that compared with the control group, the AFP level of the model group increased significantly; Compared with the model group, the AFP level of the DEHP 0.1 mg/kg group did not change significantly, while the AFP level of the DEHP 10, 1000 mg/kg group increased. Compared with the control group, the AFP level of the DEHP 1000 mg/kg control group increased significantly.

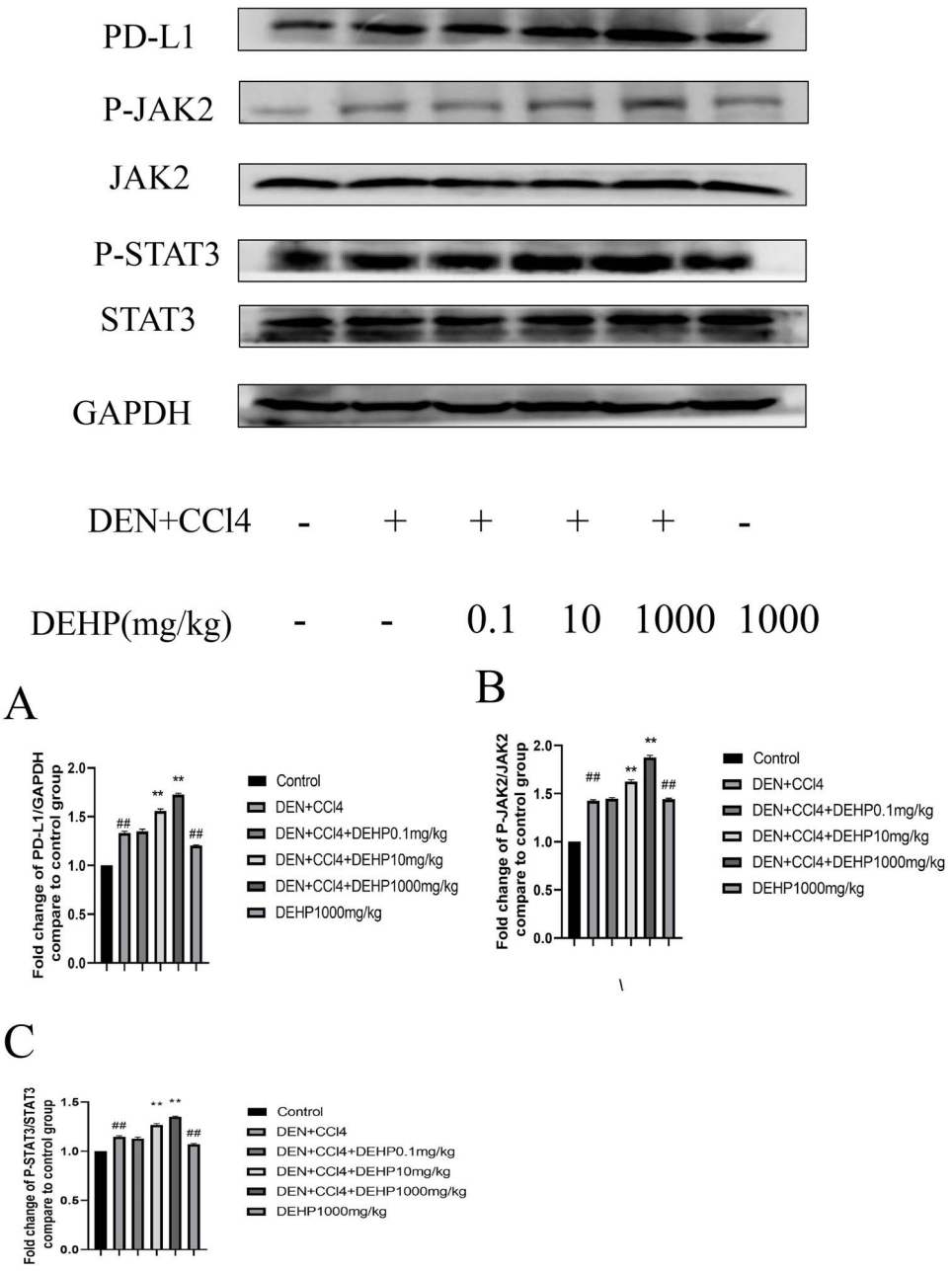

Figure 4: The effects of DEHP on the levels of (**A**) PD-L1, (**B**) P-JAK2, (**C**) P-STAT3 protein expression in the liver tissue of C57BL/6 mice (Date represent the mean ± SD, #$P < 0.05$, ##$P < 0.01$ vs. control group, *$P < 0.05$, **$P < 0.01$ vs. DEN + CCl_4 group).

The effects of DEHP on TNF-α and IL-6 in liver tissues of HCC mice

We used ELISA kits to analyze the effects of DEHP on the production of IL-6 and TNF in liver tissues. The results in Figure 2A shown that compared with the control group, the IL-6 level of the model group was significantly increased; Compared with the model group, the IL-6 level of DEHP 0.1, 10 mg/kg group did not change significantly, while the IL-6 level of DEHP 1000 mg/kg group increased significantly. Compared with the control group, the IL-6 level of the DEHP 1000 mg/kg control group was significantly increased. However, Figure 2B shown that compared with the control group, the TNF-α level of the model group increased significantly; compared with the model group, the TNF-α level of the DEHP 0.1 mg/kg group did not change significantly, while the TNF-α level of the DEHP 10, 1000 mg/kg group was significant increase. Compared with the control group, the level of TNF-α in the DEHP 1000 mg/kg control group increased significantly.

The effects of DEHP on pathological changes in mice

Use H&E staining to estimate changes in mice liver tissue structure. In Figure 2C, the liver pathological section of the mice in the normal group showed complete liver lobule structure, clear nucleus, full cytoplasm, liver cords arranged neatly, and clear boundaries. Compared with the normal group, the DEHP 1000 mg/kg control group only had unclear cell boundaries, narrow liver sinusoids, and slight inflammatory cell infiltration in the vein area. The morphology of cancer cells in model group,

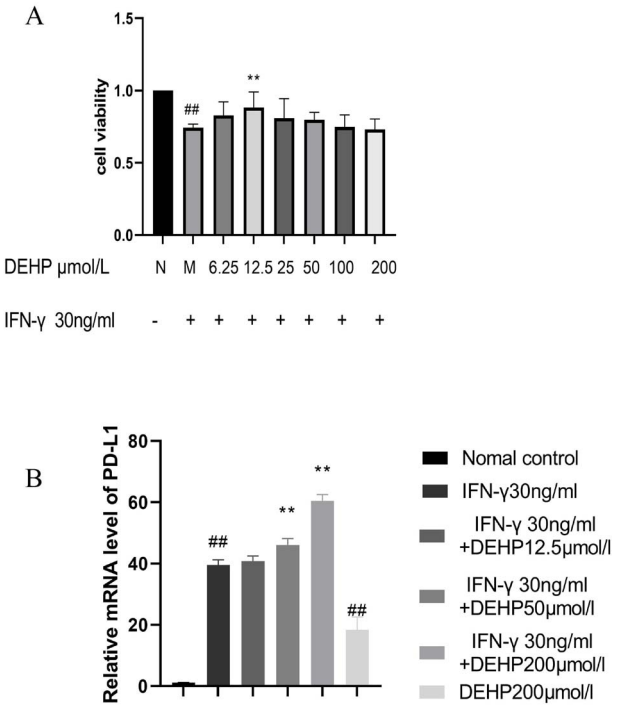

Figure 5: (**A**) The effects of DEHP on the proliferation by CCK-8 assay in HepG2 cells. (**B**) The effects of DEHP on the expression of PD-L1 mRNA in HepG2 cells was measured by RT-PCR (##$P < 0.01$ vs. normal control group, **$P < 0.01$ vs. model group).

DEHP 0.1 mg/kg group and DEHP 10 mg/kg dose group was different from that of normal liver cells. The tumor cells were arranged in thin liver plate with large cells and no obvious inner layer. The ratio of cancer cells to nucleoplasm increased slightly. However, in the dose of 1000 mg/kg DEHP, the morphology of cancer cells was significantly different from that of normal hepatocytes, with cytoplasmic decrease, large and irregular nuclei, and a significant increase in the ratio of nucleus to cytoplasm.

The effects of DEHP on laser confocal for PD-L1 expression in liver tissues

Figure 3 represented the tissue expression level of PD-L1 described by LSCM. It can be seen from Figure 3 that the PD-L1 protein increased with the increase of DEHP dose, but the expression of PD-L1 protein in DEHP 1000 mg/kg control group was not obvious.

DEHP increased the expression of PD-L1, P-JAK2, P-STAT3 protein expression in liver tissues

The expression levels of PD-L1, P-JAK2, and P-STAT3 were detected by western blotting in Figure 4. Compared with the control group, the expression of PD-L1, P-JAK2, and P-STAT3 proteins in the model group increased significantly. Compared with the model group, the expression of PD-L1, P-JAK2, and P-STAT3 proteins expressed in the DEHP 0.1 mg/kg group did not change significantly, while the expression of PD-L1, P-JAK2, and P-STAT3 expressed in the DEHP 10, 1000 mg/kg group increased significantly. Compared with the control group, the expression of PD-L1, P-JAK2, and P-STAT3 proteins in the DEHP 1000 mg/kg control group increased significantly.

The effects of DEHP on HepG2 cells viability

We evaluated its proliferation to human liver cancer cell line(HepG2) by CCK-8 assay (Fig. 5A). Compared with the normal control group, the viability of HepG2 cells was significantly decreased in the treatments with IFN-γ group. At the same time, our results indicated that a lower concentration of DEHP (12.5 μmol/l) can increase cell viability than IFN-γ group, but a higher concentration of DEHP has no significant effect on cell viability.

DEHP increased PD-L1 mRNA expression in HepG2 cells

We evaluated the effects of DEHP on PD-L1 mRNA expression by RT-PCR (Fig. 5B). Compared with the normal control group, the expression of PD-L1 mRNA in the treatments with IFN-γ group was significantly increased. At the same time, compared with the treatments with IFN-γ group, the expression of PD-L1 mRNA in the DEHP 12.5 μmol/l group did not change significantly, while the expression of PD-L1 mRNA in the DEHP 50, 200 μmol/l group increased significantly. Compared with the normal control group, the expression of PD-L1 mRNA in the DEHP200 μmol/l control group increased significantly.

The effects of DEHP on the migration of HepG2 cells

We evaluated its migration to HepG2 by transwell (Fig. 6A). Compared with the normal control group, the migration ability of HepG2 cells in the treatments with IFN-γ group was significantly reduced. Compared with the treatments with IFN-γ group, the migration ability of HepG2 cells in the DEHP 12.5, 50, 200 μmol/l groups were significantly increased. Compared with the normal control group, the migration ability of HepG2 cells in the DEHP 200 μmol/l control group was significantly increased.

The effects of DEHP on laser confocal for PD-L1 expression in HepG2 cells

Figure 6B represented cell expression level of PD-L1 as described by LSCM. It can be seen from the figure that the expression of PD-L1 protein increased with the increase of DEHP dose, but the expression of PD-L1 protein in the DEHP 200 μmol/l control group was not obvious.

DEHP increased the expression of PD-L1, P-JAK2, and P-STAT3 protein expression in HepG2 cells

In order to verify the changes in protein levels, HepG2 cells were used in *in vitro* western blot experiments. The test results of the CCK-8 kit show that low concentrations of DEHP can improve cell viability, while high concentrations of DEHP have no significant effect on cell viability. The research team chose low, medium, and high concentrations of DEHP (12.5, 50, 200 μmol/l) for *in vitro* research. As shown in Figure 7A, compared with the normal control group, the treatments with IFN-γ group showed higher PD-L1 expression. Compared with the treatments with IFN-γ group, DEHP exposure enhanced the increase in PD-L1 expression induced by IFN-γ. As shown in Figure 7B and C, the P-JAK2 and P-STAT3 proteins increased in the treatments with IFN-γ group compared to the normal control group. After exposure to DEHP, the expression of P-JAK2 and P-STAT3 proteins increased with subsequent increases in DEHP concentration.

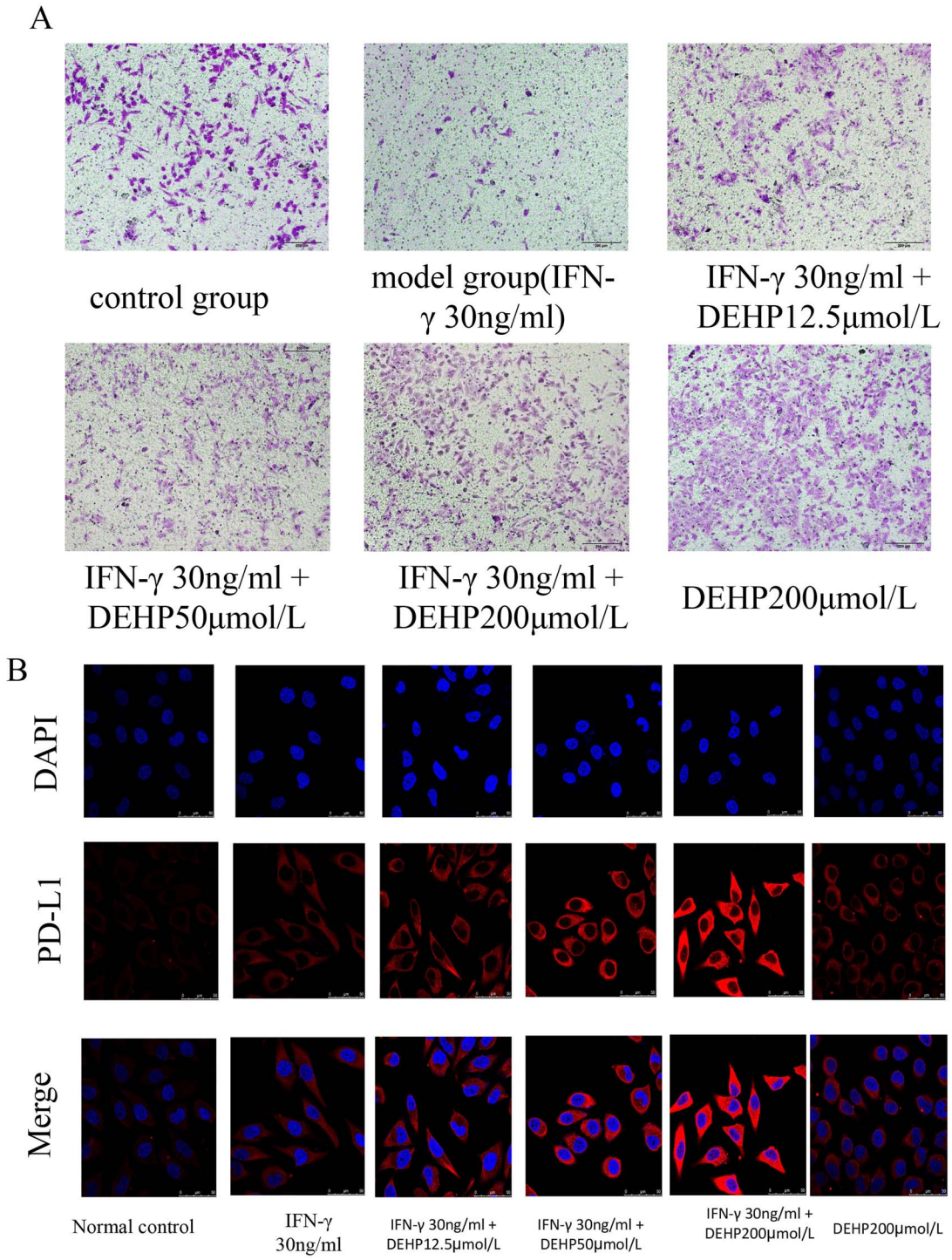

Figure 6: (**A**) The effects of DEHP on the migration by transwell in HepG2 cells. (**B**) LSCM for PD-L1 protein expression and distribution, the PD-L1 is showed red color, the nucleus blue color with DAPI.

Especially in the DEHP group of 50 and 200 μmol/l, its expression increased significantly compared with the treatments with IFN-γ group. As shown in Table 3, we summarized the results of 3.1–3.12 in a table.

Discussion

In recent years, with the continuous economic development of various countries, people are paying more and more attention to the ecological and environmental problems brought about by the economic development while developing the economy. Many studies have found that several commonly used industrial chemicals such as plasticizers and pesticides are increasingly polluting the environment. As early as 1920, people synthesized phthalates or phthalates through phthalic acid. This substance is widely used in various products, including medical equipment, cosmetics, polyvinyl chloride (PVC) flooring, food packaging, plastics

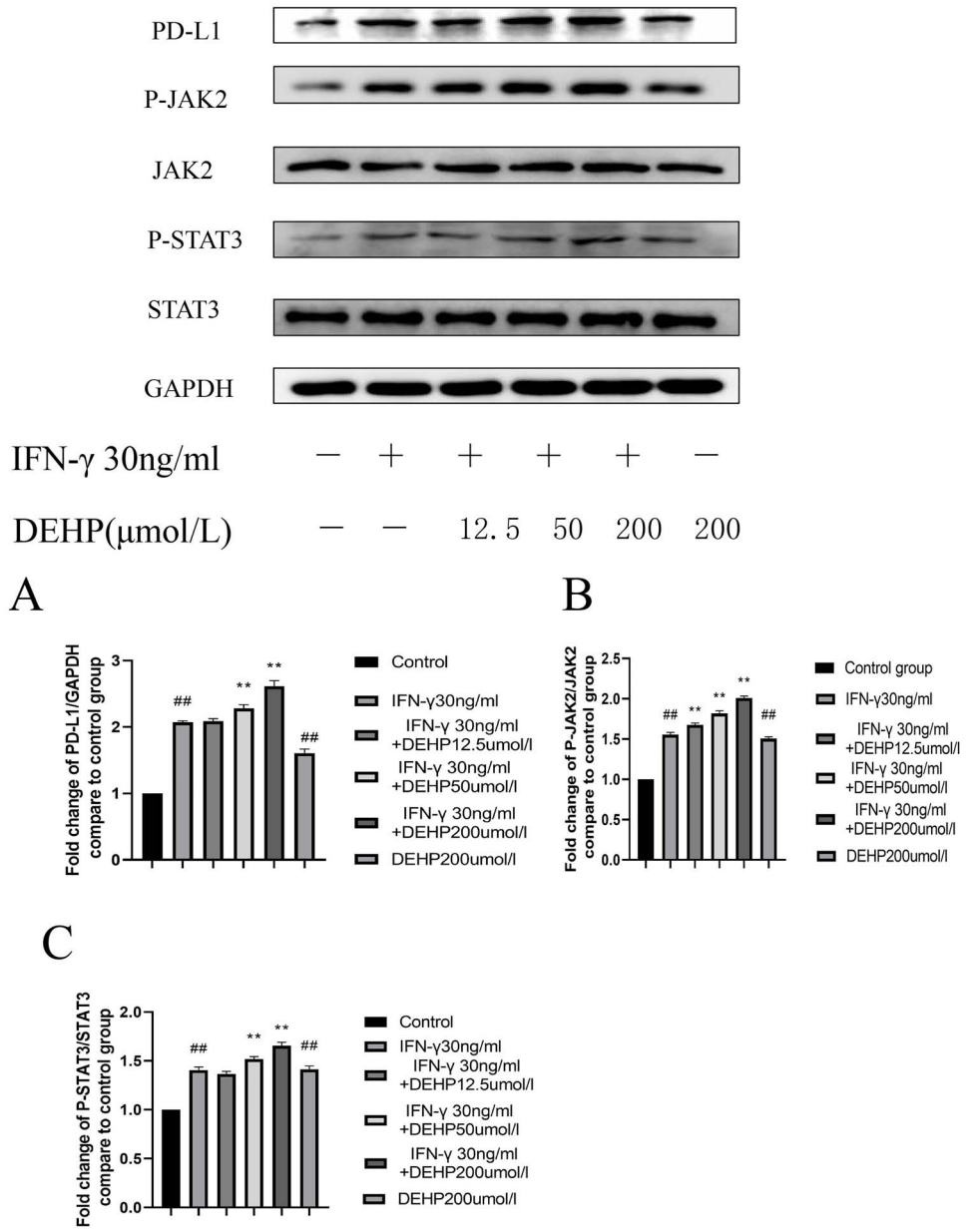

Figure 7: The effects of DEHP on the levels of (**A**) PD-L1, (**B**) P-JAK2/JAK2, (**C**) P-STAT3/STAT3 protein expression inHepG2 cells (Date represent the mean ± SD, #P < 0.05, ##P < 0.01 vs. normal control group, *P < 0.05, **P < 0.01 vs. IFN-γ group)

products, etc. [23]. Among these chemical contaminants, DEHP, which is commonly used as a plasticizer for PVC, has been reported most recently [24]. People are constantly researching and discovering that the chronic exposure levels considered to be tolerable to the general population, namely the reference dose (RFD) of the US Environmental Protection Agency (USEPA) and the tolerable daily intake (TDI) of the EU, are respectively 20 and 37 μg/kg body weight/day [25]. In addition, people will also be exposed to higher doses of DEHP during certain medical procedures, including gastric tubes, dialysis, infusion bags, and so on [26]. As a widely used endocrine disruptor, DEHP has received extensive attention due to its potential toxic effects. The health hazards to the human body include carcinogenicity, kidney and liver damage, reproductive toxicity, and endocrine disorders [27]. In addition, studies have shown that DEHP can induce hepatotoxicity in quail by regulating the mitochondrial unfolded protein response and NRF2-mediated antioxidant defense [28]. There is also a report that DEHP can promote oxidative stress, disrupt the balance of the antioxidant system, up-regulate the TGF-β1/Smad and p38MAPK/NF-κB signaling pathways, thereby promoting the development of liver fibrosis [20]. After the human body is exposed to DEHP, when DEHP enters the human body through liver metabolism, its short-term toxicity may not be obvious, but over time, various toxicities may appear, and the accumulation of toxicity persists. It should be emphasized that if the liver is in a certain disease state or in the stage of disease development and occurrence, the toxicity of DEHP can be amplified or participate in the occurrence of the disease. In this study, we linked DEHP to the formation of HCC to explore the effect of DEHP on HCC.

DEHP is a plasticizer widely used in various commercial products, which has potential carcinogenic effects [29]. According to

Table 3: Summary of the results of sections 3.1–3.12

	Control	Model (DEN + CCl_4)	DEN + CCl_4 + DEHP 0.1 mg/kg	DEN + CCl_4 + DEHP 10 mg/kg	DEN + CCl_4 + DEHP 1000 mg/kg	DEHP 1000 mg/kg
Liver index (g/100 g)	4.87 ± 0.35	5.93 ± 0.47**	6.03 ± 0.59	6.80 ± 0.45****	8.09 ± 0.62****	6.96 ± 0.70**
Tumor size (mm)	—	5.98 ± 0.38	6.23 ± 0.37	6.80 ± 0.66****	10.90 ± 1.17***	—
Tumor number	—	10 ± 0.71	10 ± 1.41	11 ± 1.58	17.75 ± 1.09****	—
AST (U/L)	11.91 ± 2.25	64.64 ± 6.93**	64.19 ± 6.63	69.96 ± 4.90	104.42 ± 9.15****	28.88 ± 5.05*
ALT (U/L)	6.38 ± 1.19	56.92 ± 4.90**	56.27 ± 5.89	61.04 ± 5.75	80.75 ± 6.53****	17.79 ± 4.06*
AFP (ng/ml)	5.41 ± 0.74	15.28 ± 1.49**	16.01 ± 1.20	16.46 ± 1.58	20.37 ± 1.61****	8.44 ± 0.77*
TNF-α (pg/ml)	5.24 ± 0.25	16.48 ± 0.93**	17.32 ± 1.06	18.41 ± 0.75	22.69 ± 1.65****	10.66 ± 0.75**
IL-6 (pg/ml)	4.37 ± 0.91	15.21 ± 1.25**	15.79 ± 1.21	16.36 ± 0.53	20.78 ± 1.36****	8.60 ± 0.73*

Date represent the mean ± SD.
*$P < 0.05$.
**$P < 0.01$ vs. control group.
***$P < 0.05$.
****$P < 0.01$ vs. DEN + CCl_4 group.

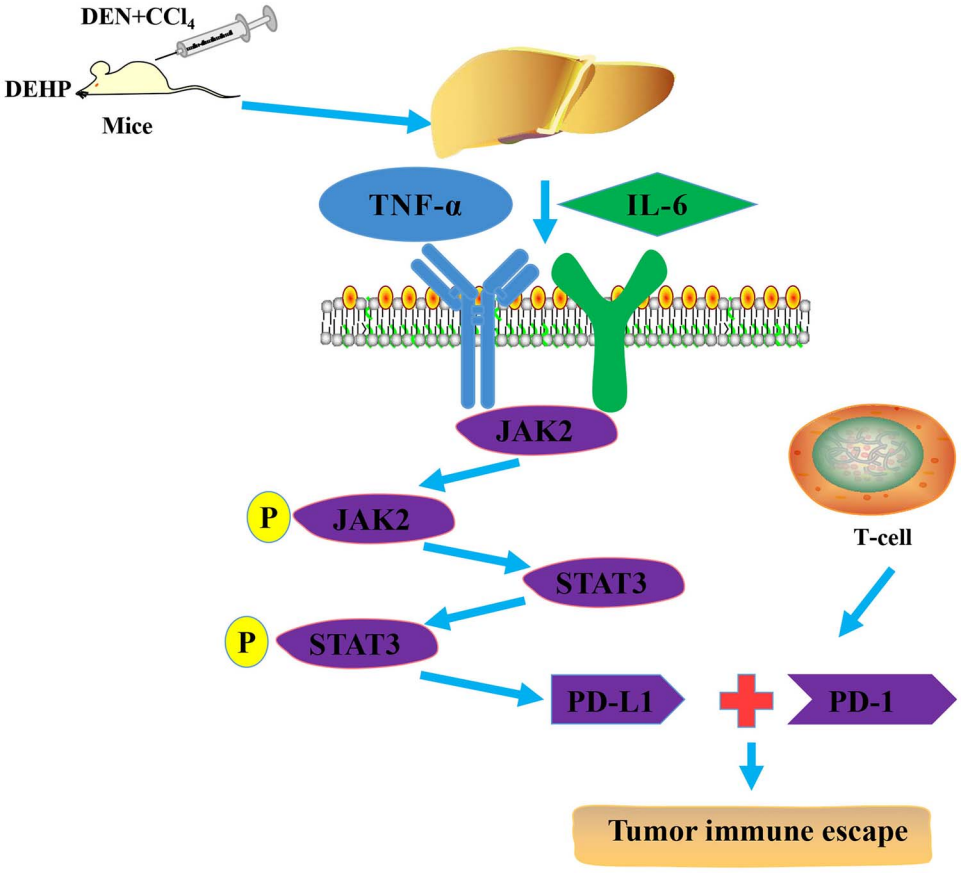

Figure 8: DEHP may be involved in the pathological process of HCC. DEHP increased the expression of IL-6 and TNF-α and effects the JAK2/STAT3 signaling pathway. When IL-6 and TNF-α bind to their transmembrane receptors, JAK2 and STAT3 are activated, and DEHP activated the JAK2/STAT3 signaling pathway, promoted the expression of PD-L1, and then promoted tumor immune escape response

the results of classic biochemical indicators, under the action of plasticizers, the serum ALT and AST levels of HCC mice were significantly increased, and the liver index was increased with weight loss, indicating that the mice may be in a state of severe liver damage. This study showed that low-dose DEHP has an effect on cell viability of HepG2 cells, while high-dose DEHP has no significant effect on cell viability, as shown by the CCK analysis results. In order to support the proliferation effect of DEHP, the study pointed out that DEHP can promote the expression of TNF-α in the liver tissue of HCC mice. The cytokine regulates various biological processes, including cell proliferation and the production of inflammatory mediators [30]. In addition, the sustained release of TNF-α is related to the induction of signal transduction pathways involved in tumor progression, such as JAK/STAT signal transduction [31, 32]. According to our results, high-dose DEHP can significantly promote the expression of TNF-α. Consistent with these results, recent evidence suggests the role of TNF-α in the poor prognosis of patients with liver

cancer. IL-6 is an inflammatory cytokine produced by lymphoid and non-lymphoid cells. It has important immunological activity. Its high expression is related to inflammation-related diseases and participates in the occurrence and development of chronic liver disease and liver cancer [33–35]. IL-6 is an important extracellular factor in the Jak/Stat signaling pathway, and its increase also activates the JAK/STAT signaling pathway, which promotes tumor proliferation and development [36, 37]. This experiment found that the level of IL-6 in HCC mice increased significantly, and the level of IL-6 in DEHP middle and high dose groups increased. DEHP may play a role in promoting tumors by affecting the tumor inflammatory microenvironment.

Tumor immune escape refers to the phenomenon that tumor cells grow and metastasize through various mechanisms to avoid the recognition and attack of the immune system. It is an important strategy for tumor survival and development. The PD-L1/PD-1 signaling pathway is an important part of tumor immunosuppression. PD-L1 is expressed on immune cells and a variety of cancer cells (including liver cancer), PD-L1 molecules on malignant cells can bind to its receptor PD-1, which can inhibit the activation of T lymphocytes and T cells, enhance tumor cell tolerance and immune tolerance, thereby achieving tumor immune escape [15, 38]. Various signal pathways can regulate the expression of PD-L1.The JAK/STAT signal transduction pathway is a classic way to link inflammation with tumorigenesis. The activation of JAK/STAT signal promotes tumor growth and invasion and immunosuppression. In addition, it is reported that PD-L1 is one of the hot spots in current immunotherapy, and in many cell types, it is regulated by JAK/STAT signals, especially JAK2/STAT3 [39]. In addition, DEHP has also been reported to activate JAK2/STAT3 activity. Studies have reported that DEHP can regulate myocardial hypertrophy induced by IL-6/JAK/STAT3 pathway [40]. In addition, a study found that DEHP may induce glucose metabolism disorders in adolescent rats by interfering with the JAK2/STAT3 pathway, and regulate the sensitivity of insulin receptors and leptin receptors [41]. In *in vivo* experiments, western blot analysis showed that DEHP increased the expression of PD-L1, P-JAK2, and P-STAT3. At the same time, *in vitro* experiments, we got the same result. Therefore, we can preliminarily conclude that DEHP may promote the expression of PD-L1 by activating JAK2/STAT3.

Conclusion

Our research showed that DEHP significantly increases the severity of HCC induced by DEN combined with CCl_4 by promoting tumor immune escape response. *In vivo* experimental data show that DEHP can significantly increase the expression of PD-L1 and inhibit anti-tumor immunity, which may be mediated by up-regulating the level of JAK2/STAT3. *In vitro* experiment, we demonstrated that IFN-γ can activate STAT3 in HepG2 cells, and this stimulation is further enhanced by DEHP, which leads to increased expression of PD-L1 in HepG2 cells, and ultimately reduces the sensitivity of tumor cells to CTL (Fig. 8). Exposure to DEHP for a long time may cause its toxicity to accumulate, thereby promoting the occurrence and development of various potential diseases. Therefore, it is important to study the effects of DEHP toxicity on humans. As shown in this study, DEHP plays an important role in the formation and development of HCC, and its potential harm deserves further research and attention. Finally, the results of this research provide that the toxic effect of plasticizer (DEHP) in HCC needs to be paid attention to and is of great significance for the prevention and treatment of HCC in the future.

Authors' contributions

Q.X. and S.H. contributed for investigation; Q.X., S.H., Z.X., and K.J. for methodology; S.H. and X.Z. for resources; W.W. and W.X. for supervision; Q.X. for writing original draft; and W.W. and W.X. for writing, reviewing, and editing the article.

Acknowledgments

This work was funded by the Anhui Natural Science Foundation Project (China, No. 1608085MH176) and National Natural Science Foundation Project (China, No. 51672004).

Conflict of interest statement

The authors declare that they have no competing interests regarding this study.

Abbreviations

DEHP, di(2-ethylhexyl) phthalate; HCC, hepatocellular carcinoma; PD-L1, programmed cell death 1 ligand 1; JAK2, Janus Kinase 2; STAT3, signal transducer and activator of transcription; DEN, diethylnitrosamine; CCl_4, carbon tetrachloride; AST, aspartate aminotransferase; ALT, alanine aminotransferase; AFP, alpha-fetoprotein; TNF-α, tumor necrosis factor α; IL-6, interleukin-6; PD-1, programmed cell death protein 1; CTL, cytotoxic lymphocyte; RIPA, Radio-Immunoprecipitation Assay; BCA, Bicichoninic ccid; PVDF, Polyvinylidene fluoride; TPBS, Tween phosphate buffer saline.

References

1. Du P, Huang Y, Lü H *et al.* Rice root exudates enhance desorption and bioavailability of phthalic acid esters (PAEs) in soil associating with cultivar variation in PAE accumulation. *Environ Res* 2020;**186**:109611.
2. Hamid N, Junaid M, Manzoor R *et al.* Prioritizing phthalate esters (PAEs) using experimental in vitro/vivo toxicity assays and computational in silico approaches. *J Hazard Mater* 2020;**398**:122851.
3. Khasin LG, Della Rosa J, Petersen N *et al.* The impact of di-2-ethylhexyl phthalate on sperm fertility. *Front Cell Dev Biol* 2020;**8**:426.
4. Ramadan M, Cooper B, Posnack NG. Bisphenols and phthalates: plastic chemical exposures can contribute to adverse cardiovascular health outcomes. *Birth Defects Res* 2020;**10**:1002.
5. Zhang X, Zhao Y, Cheng C *et al.* Combined effects of di(2-ethylhexyl) phthalate and bisphenol A on thyroid hormone homeostasis in adolescent female rats. *Environ Sci Pollut Res Int* 2020;**27**:40882–92.
6. Lee C, Suk F, Twu Y *et al.* Long-term exposure to low-dose di-(2-ethylhexyl) phthalate impairs cholesterol metabolism in hepatic stellate cells and exacerbates liver fibrosis. *Int J Env Res Public Health* 2020;**17**:3802.
7. Benjamin S, Masai E, Kamimura N *et al.* Phthalates impact human health: epidemiological evidences and plausible mechanism of action. *J Hazard Mater* 2017;**340**:360–83.
8. Lu Y, Yao G, Wang X *et al.* A comprehensive analysis of metabolomics and transcriptomics reveals new biomarkers and mechanistic insights on DEHP exposures in MCF-7 cells. *Chemosphere* 2020;**255**:126865.

9. Cheng C, Shou Q, Lang J *et al*. Gehua Jiecheng decoction inhibits diethylnitrosamine-induced hepatocellular carcinoma in mice by improving tumor immunosuppression microenvironment. *Front Pharmacol* 2020;**11**:809.
10. Dong L, Yu L, Li H *et al*., An NAD(+)-dependent deacetylase SIRT7 promotes HCC development through deacetylation of USP39. *iScience* 2020;**23**:101351.
11. Lim JY, Liu C, Hu KQ *et al*. Xanthophyll β-cryptoxanthin inhibits highly refined carbohydrate diet–promoted hepatocellular carcinoma progression in mice. *Mol Nutr Food Res* 2020;**64**:1900949.
12. Zheng L, Li C, Huang X *et al*. Thermosensitive hydrogels for sustained-release of sorafenib and selenium nanoparticles for localized synergistic chemoradiotherapy. *Biomaterials* 2019;**216**:119220.
13. Choi J, Jo C, Lim YS. Tenofovir vs. entecavir on recurrence of hepatitis B virus-related hepatocellular carcinoma after surgical resection. *Hepatology* 2020;**10**:1002.
14. Zhu K, Huang W, Wang W *et al*. Up-regulation of S100A4 expression by HBx protein promotes proliferation of hepatocellular carcinoma cells and its correlation with clinical survival. *Gene* 2020;**749**:144679.
15. Jiang X, Wang J, Deng X *et al*. Role of the tumor microenvironment in PD-L1/PD-1-mediated tumor immune escape. *Mol Cancer* 2019;**18**:10.
16. Noguchi T, Ward JP, Gubin MM *et al*. Temporally distinct PD-L1 expression by tumor and host cells contributes to immune escape. *Cancer Immunol Res* 2017;**5**:106–17.
17. Kim DH, Kim H, Choi YJ *et al*. Exosomal PD-L1 promotes tumor growth through immune escape in non-small cell lung cancer. *Exp Mol Med* 2019;**51**:1–13.
18. Yasuoka H, Asai A, Ohama H *et al*. Increased both PD–L1 and PD-L2 expressions on monocytes of patients with hepatocellular carcinoma was associated with a poor prognosis. *Sci Rep-Uk* 2020;**10**:10377.
19. Sangro B, Melero I, Wadhawan S *et al*. Association of inflammatory biomarkers with clinical outcomes in nivolumab-treated patients with advanced hepatocellular carcinoma. *J Hepatol* 2020;**73**:1460–9 [published online ahead of print, 22 July 2020] S0168-8278(20)30479-7.
20. Zhao Z, Ji K, Shen X *et al*. Di(2-ethylhexyl) phthalate promotes hepatic fibrosis by regulation of oxidative stress and inflammation responses in rats. *Environ Toxicol Phar* 2019;**68**: 109–19.
21. Li Z, Li B, Li L *et al*. The immunostimulative effect and mechanisms of a novel mouse anti-human PD-1 monoclonal antibody on Jurkat lymphocytic cells cocultured with hepatoma cells. *Onco Targets Ther* 2020;**13**:12225–41.
22. Banales JM, Iñarrairaegui M, Arbelaiz A *et al*. Serum metabolites as diagnostic biomarkers for cholangiocarcinoma, hepatocellular carcinoma, and primary sclerosing cholangitis. *Hepatology* 2019;**70**:547–62.
23. Kimber I, Dearman RJ. An assessment of the ability of phthalates to influence immune and allergic responses. *Toxicology* 2010;**271**:73–82.
24. Fréry N, Santonen T, Porras SP *et al*. Biomonitoring of occupational exposure to phthalates: a systematic review. *Int J Hyg Environ Health* 2020;**229**:113548.
25. Chen M, Chen J, Tang C *et al*. The internal exposure of Taiwanese to phthalate—an evidence of intensive use of plastic materials. *Environ Int* 2008;**34**:79–85.
26. Bouattour Y, Wasiak M, Bernard L *et al*. Quantification of bis(2-ethylhexyl) phthalate released by medical devices during respiratory assistance and estimation of patient exposure. *Chemosphere* 2020;**255**:126978.
27. Ishii S, Katagiri R, Minobe Y *et al*. Investigation of the amount of transdermal exposure of newborn babies to phthalates in paper diapers and certification of the safety of paper diapers. *Regul Toxicol Pharmacol* 2015;**73**:85–92.
28. Zhang Q, Zhao Y, Talukder M *et al*. Di(2-ethylhexyl) phthalate induced hepatotoxicity in quail (*Coturnix japonica*) via modulating the mitochondrial unfolded protein response and NRF2 mediated antioxidant defense. *Sci Total Environ* 2019;**651**:885–94.
29. Crobeddu B, Ferraris E, Kolasa E *et al*. Di(2-ethylhexyl) phthalate (DEHP) increases proliferation of epithelial breast cancer cells through progesterone receptor dysregulation. *Environ Res* 2019;**173**:165–73.
30. Matsumoto J, Dohgu S, Takata F *et al*. TNF-α-sensitive brain pericytes activate microglia by releasing IL-6 through cooperation between IκB-NFκB and JAK-STAT3 pathways. *Brain Res* 2018;**1692**:34–44.
31. Gulluoglu S, Tuysuz EC, Sahin M *et al*. The role of TNF-α in chordoma progression and inflammatory pathways. *Cell Oncol* 2019;**42**:663–77.
32. Chen M, Zeng J, Chen S *et al*. SPTBN1 suppresses the progression of epithelial ovarian cancer via SOCS3-mediated blockade of the JAK/STAT3 signaling pathway. *Aging (Albany NY)* 2020;**12**:10896–911.
33. Čokić VP, Mitrović-Ajtić O, Beleslin-Čokić BB *et al*. Proinflammatory cytokine IL-6 and JAK-STAT Signaling pathway in myeloproliferative neoplasms. *Mediators Inflamm* 2015;**2015**:453020.
34. Lai S, Su Y, Chi C *et al*. DNMT3b/OCT4 expression confers sorafenib resistance and poor prognosis of hepatocellular carcinoma through IL-6/STAT3 regulation. *J Exp Clin Cancer Res* 2019;**38**:474.
35. Lin Y, Yang X, Liu W *et al*. Chemerin has a protective role in hepatocellular carcinoma by inhibiting the expression of IL-6 and GM-CSF and MDSC accumulation. *Oncogene* 2017;**36**:3599–608.
36. Cheteh EH, Sarne V, Ceder S *et al*. Interleukin-6 derived from cancer-associated fibroblasts attenuates the p53 response to doxorubicin in prostate cancer cells. *Cell Death Dis* 2020;**6**:42.
37. Yoshida GJ. Regulation of heterogeneous cancer-associated fibroblasts: the molecular pathology of activated signaling pathways. *J Exp Clin Cancer Res* 2020;**39**:1–15.
38. Ke M, Zhang Z, Xu B *et al*. Baicalein and baicalin promote antitumor immunity by suppressing PD-L1 expression in hepatocellular carcinoma cells. *Int Immunopharmacol* 2019; **75**:105824.
39. Zhang W, Liu Y, Yan Z *et al*. IL-6 promotes PD-L1 expression in monocytes and macrophages by decreasing protein tyrosine phosphatase receptor type O expression in human hepatocellular carcinoma. *J Immunother Cancer* 2020;**8**:e000285.
40. Cai J, Shi G, Zhang Y *et al*. Taxifolin ameliorates DEHP-induced cardiomyocyte hypertrophy via attenuating mitochondrial dysfunction and glycometabolism disorder in chicken. *Environ Pollut* 2019;**255**:113155.
41. Xu J, Zhou L, Wang S *et al*. Di-(2-ethylhexyl)-phthalate induces glucose metabolic disorder in adolescent rats. *Environ Sci Pollut R* 2018;**25**:3596–3607.